Unclassified
SECURITY CLASSIFICATION OF THIS PAGE

REPORT DOCUMENTATION PAGE

Form Approved
OMB No. 0704-0188

1a. REPORT SECURITY CLASSIFICATION Unclassified	1b. RESTRICTIVE MARKINGS
AD-A224 281	3. DISTRIBUTION/AVAILABILITY OF REPORT Approved for public release; distribution is unlimited.
4. PERFORMING ORGANIZATION REPORT NUMBER(S)	5. MONITORING ORGANIZATION REPORT NUMBER(S) AFOSR-TR- 90 0748
6a. NAME OF PERFORMING ORGANIZATION Princeton University 6b. OFFICE SYMBOL (If applicable)	7a. NAME OF MONITORING ORGANIZATION AFOSR/NA
6c. ADDRESS (City, State, and ZIP Code) Princeton, NJ 08544	7b. ADDRESS (City, State, and ZIP Code) Building 410, Bolling AFB DC 20332-6448
8a. NAME OF FUNDING/SPONSORING ORGANIZATION AFOSR/NA 8b. OFFICE SYMBOL (If applicable) NA	9. PROCUREMENT INSTRUMENT IDENTIFICATION NUMBER AFOSR 89-0293
8c. ADDRESS (City, State, and ZIP Code) Building 410, Bolling AFB DC 20332-6448	10. SOURCE OF FUNDING NUMBERS PROGRAM ELEMENT NO. 61102F; PROJECT NO. 2308; TASK NO A2; WORK UNIT ACCESSION NO.

DTIC ELECTE JUL 20 1990 S F

11. TITLE (Include Security Classification)
(U) Chemical Kinetic and Aerodynamic Structures of Flames

12. PERSONAL AUTHOR(S)
C.K. Law

13a. TYPE OF REPORT	13b. TIME COVERED	14. DATE OF REPORT (Year, Month, Day)	15. PAGE COUNT
Annual Report	FROM 89-03-01 TO 90-02-28	90-06-20	27

16. SUPPLEMENTARY NOTATION

17. COSATI CODES			18. SUBJECT TERMS (Continue on reverse if necessary and identify by block number)
FIELD	GROUP	SUB-GROUP	Flame Dynamics, Flame Kinetics, Turbulent Flames, Soot Formation, Flammability Limits

19. ABSTRACT (Continue on reverse if necessary and identify by block number)

During the reporting period extensive experimental and numerical studies on the dynamics and kinetics of laminar premixed and diffusion flames have been conducted. Specific problems investigated include dilution and temperature effects in soot formation in diffusion flames, chemical and physical effects of additives in soot formation, experimental determination of laminar flame speeds of ethane, ethylene, acetylene, propane and hydrogen mixtures with air and the partial validation of the associated kinetic mechanisms, the theoretical prediction and experimental determination of the flammability limits of a variety of combustible mixtures, and the determination of the dynamic and chemical kinetic structures of diffusion flames near extinction. A total of seven journal-class publications resulted from these investigations.

20. DISTRIBUTION/AVAILABILITY OF ABSTRACT	21. ABSTRACT SECURITY CLASSIFICATION
☒ UNCLASSIFIED/UNLIMITED ☒ SAME AS RPT ☐ DTIC USERS	Unclassified
22a. NAME OF RESPONSIBLE INDIVIDUAL Julian M Tishkoff	22b. TELEPHONE (Include Area Code) (202) 767-4935
	22c. OFFICE SYMBOL AFOSR/NA

DD Form 1473, JUN 86 Previous editions are obsolete. SECURITY CLASSIFICATION OF THIS PAGE

Unclassified

1. Introduction

During the reporting period studies have been conducted in two major areas in fundamental combustion, namely soot formation and the structure of laminar flames. Concerning soot formation, the emphasis has been on further resolving the relative importance of temperature versus dilution in soot formation. As a companion project, we have also identified the dominant physical and chemical influences when a certain additive, say carbon dioxide, is added to either the fuel or the oxidizer side of the flame. On flame structure studies, investigations have been conducted on premixed flames, on diffusion flames, and on the concept of flammability limits. For premixed flames, emphasis has been on the determination of the laminar flame speeds and the validation or identification of the associated chemical kinetics for the mixture of interest. Studies have been conducted on all of the C_2 fuels as well as hydrogen. For diffusion flames, we have examined the accuracies of the various descriptions of the flow fields governing counterflow diffusion flames. The study further indicates the importance of the strain rate experienced by the reaction zone of the flame in causing extinction. Concerning flammability limits, a kinetic criterion has been proposed from which the rich and lean flammability limits of a fuel-oxidizer system can be predicted from first principles. Agreement between predictions and experimental data has been extremely close, indicating the possibility that the flammability limits are kinetically controlled, and that these limits can be predicted. If what we have found is indeed correct, after further testings, it will be a significant milestone in fundamental as well as in practical combustion.

The various projects are briefly discussed in the following. Complete manuscripts have been separately submitted to the program manager.

2. Dilution Effects in Soot Formation in Diffusion Flames

A major concept developed in recent studies on soot formation in diffusion flames is that the flame temperature exerts the dominant influence on soot formation. This concept has been experimentally investigated by lowering the flame temperature by diluting the fuel stream with an inert.

In a previous study of ours we challenged this concept by suggesting that fuel dilution, in addition to the lowering of the flame temperature, could also be responsible in reducing the amount of soot formation, and that previous studies were not sufficiently well controlled because the methodology involved the simultaneous variation in the fuel concentration as well as the flame temperature.

Subsequently we proposed an alternate methodology through which temperature and concentration variations can be separately imposed. The methodology involves controlling the flame temperature by substituting a given amount of the nitrogen in the oxidizer by an equal amount of argon, which has a different specific heat. Thus the concentrations of the fuel and oxidizer streams can be held fixed while the flame temperature is changed. Consequently we demonstrated that not only temperature and dilution are both important in soot formation, in many instances dilution can be even more important. This methodology has now been termed as the heat capacity technique.

Our previous experiments were conducted by using the counterflow flame while most of the literature experiments were performed with the co-flow flame. Thus reservations have been raised concerning the applicability of our results to those of the co-flow flames. Thus in this study we have applied the heat capacity technique to identify the separate influences of temperature and dilution. Figure 1 shows the integrated soot volume fraction as a function of the axial position. Curve A has

100% C_2H_4, Curve B 50%C_2H_4/50%N_2, and Curve is the same as Curve B except the flame temperature has been adjusted to be equal to that of Curve A. Thus a comparison between Curves B and C shows the effects due to temperature variation because they have the same concentration but different temperatures, while a comparison between between Curves C an A shows the effects due to concentration variation because they have the same temperature but different concentrations. The results are qualitatively similar to what was observed with the counterflow flame, and dramatically demonstrate the fact that dilution can exert a much stronger effect than temperature in soot formation.

This work is reported in Publication No. 2.

We mention in passing that recent studies by Naegeli at the Southwest Research Institute and Gulder in Canada on premixed flames have also substantiated our contention that dilution is an important factor in soot formation in flames.

3. Effects of Additives in Soot Formation

The use of gaseous additives has been frequently suggested as a viable strategy to reduce soot formation. The cause for such a reduction, however, has not been adequately and systematically studied. Take CO_2 as an example because of its potential for implementation through exhaust gas recirculation. When CO_2 is added to a fuel or oxidizer stream, both the flame temperature and the reactant concentration are reduced, as just mentioned. CO_2, however, can also participate chemically in the soot formation process. Thus a viable study of additive effects must necessarily identify the separate effects of temperature reduction, reactant dilution, and direct chemical participation.

Figure 2 shows typical results obtained for CO_2 addition to the

fuel stream in C_2H_4 flames. Here we have used a counterflow flame and have plotted the soot particle inception limit versus the additive mole fraction. The results were obtained in the following manner. First, the soot inception limits for various amounts of fuel dilution were obtained. The experiments were repeated, for a given amount of fuel dilution, by replacing a portion of the nitrogen in the oxidizer with an equal molar amount of argon so that the flame temperature was that of the pure fuel. The difference then indicates the thermal effect of the additive.

We next replaced CO_2 by equal molar amounts of N_2, and readjust the flame temperature back to that of the pure fuel. The additional difference observed then gives the chemical effect. Finally, the difference between this result and that obtained without any dilution yields the influence of dilution. We have therefore succeeded in isolating the individual effects of dilution, temperature, and direct chemical participation. It is clear that each of these effects accounts for a measurable reduction in soot formation and therefore cannot be neglected.

This work is reported in Publication No. 3.

4. Flame Speeds and Oxidation Kinetics of C_2-Hydrocarbons

In our previous work for OSR we have developed an experimental method through which laminar flame speeds of gaseous combustibles can be accurately determined. The method involves determining the flame speeds of strained flames situated in counterflows whose strain rates can be measured. By plotting the strained flame speed versus the strain rate, the unstrained laminar flame speed can be determined through extrapolation to zero stretch. This is a significant advancement because practically all previous methods used for the determination of laminar flame speeds have flame stretch effects.

Accurate values of laminar flame speeds are needed in many aspects of fundamental and practical research. One recent use is the partial validation and/or determination of the chemical kinetic mechanisms for the oxidation of given fuel systems. It is obvious that such an effort is meaningful only if accurate experimental values of the laminar flame speeds are available.

We have previously determined the laminar flame speeds and the kinetic scheme of methane/oxygen mixtures over extensive ranges of concentration, pressure, and flame temperature. In the present study we have extended the investigation to cover all the C_2 hydrocarbon species of ethane, ethylene, and acetylene, as well as propane. Such an extension is crucial because methane only has C-H bonds while the breaking of the C_2 bonds is important in the kinetics of all of the higher hydrocarbons. Through this study we have found that all of the existing C_2 kinetic schemes are inadequate to describe our experimental result. Consequently we proposed a new scheme which was able to predict practically all of our experimental data. Figure 3 shows the comparison between experimental and calculated laminar flame speeds for ethane, ethylene, and acetylene over extensive ranges of equivalence ratios and under 1 atmosphere pressure. The agreement can be considered to be quite satisfactory.

This work is reported in Publication No. 4.

5. Flame Speeds and Oxidation Kinetics of Hydrogen

Recent interests in supersonic combustion have identified the importance of flame stabilization and hydrogen oxidation kinetics. Further discussions with chemical kineticists have convince us that the hydrogen oxidation kinetics is far from being established, especially for the very weakly-burning situations with low flame temperatures. This is certainly disturbing because hydrogen, being the simplest fuel molecule, forms the building

block for the oxidation of all hydrocarbons. Furthermore, the weakly-burning situations are relevant to ignition, extinction, flame stabilization, engine knock, etc.

A detailed literature survey then shows that there has not been many attempts at determining the laminar flame speeds of ultra lean hydrogen/air mixtures. The difficulty here is that lean hydrogen/air flames are prone to diffusional-thermal cellular instability. Consequently smooth flames have not been observed. Further recognizing the highly diffusive nature of hydrogen and its strong influence by stretch, the usefulness of the previous data on lean hydrogen-air flame speed is in question.

In this study we have therefore accurately determined the laminar flame speeds of hydrogen/air mixtures over extensive variations of the equivalence ratio and pressure. A comparison of these data with calculated values using different literature kinetic schemes reveal the inadequacy of existing mechanisms under low flame temperatures. Figure 4 shows that the experimental values are consistently higher than the calculated values. Systematic sensitivity analysis and adjustment of kinetic parameters fail to improve the discrepancy. It is therefore believe that there is a missing channel of chain branching which has not been identified.

This work is reported in Publication No. 5.

6. Flammability Limits

An unsolved problem in fundamental combustion research is the meaning and possible existence of flammability limits. Empirically, it has been observed that a particular fuel/oxidizer system becomes absolutely noncombustible when its (fuel) concentration is beyond either a lean or a rich limit. For example, for the methane/air system, the lean and rich limits are respectively 4.8 and 15% of methane. The confusion governing

flammability limits is that: (a) It is not sure whether flammability limit indeed exists; (b) What is the mechanism governing its onset if it exists; and (c) How can it be predicted from first principles?

In the present investigation we have first conceptually defined the phenomenon of flammability limit as the mixture concentration beyond which steady propagation of an adiabatic, planar, flame becomes impossible. Clearly, if a flame cannot propagate in such an idealized mode, it will not be able to propagate in other nonadiabatic situations. Next, in order to quantitatively determine a flammability limit from first principles, we identify a limit as the state at which the termination reaction of a crucial chain branching-termination reaction pair becomes more sensitive to changes in the mixture concentration than the corresponding branching reaction. Thus as long as the kinetic mechanism of the fuel/oxidizer system is known, the state of flammability can be predicted. Finally, we have also experimentally determined the flammability limits of a great variety of mixtures by first determining the extinction limits of an adiabatic stretched flame, and then extrapolating the results to zero stretch.

Table 1 shows the presently determined theoretical and experimental flammability limits in terms of the fuel concentration (Ω^*) and equivalence ratio (ϕ^*). Figure 5 compares the theoretical and experimental limits. The closeness of the comparison is quite evident. The study further identifies many properties of the flammability limits.

This work is reported in Publication No. 6.

7. Extinction of Methane/Air Diffusion Flames by Stretch

Although extensive amount of work has been performed on the

structure and extinction of laminar diffusion flames, there does not exist any quantitative experimental data on the flame structure determined by using laser techniques. Thus in the present investigation we have first accurately determined the velocity structure of counterflow diffusion flames by using LDV, especially for states close to extinction. These profiles are then compared with numerically-calculated ones with different descriptions of the flow field. Figure 6 shows that the comparison is quite good if the flow field is described by the plug flow. It is further found that the maximum velocity gradient, which occurs on the fuel side of the main reaction zone, achieves a value at extinction that is relatively insensitive to the boundary conditions of the flow.

This work is reported in Publication No. 7.

8. List of Publications

1. "Chain Mechanisms in the Overall Reaction Orders in Laminar Flame Propagation," by F.N. Egolfopoulos and C.K. Law, Combustion and Flame 80: 7-16 (1990).**Attached as Appendix A**

2. "Soot Formation and Inert Addition in Diffusion Flames," by R.L. Axelbaum and C.K.Law, to appear in Proc. of 23rd Combustion Symposium.

3. "The Influence of Carbon Dioxide and Oxygen as Additives on Soot Formation in Diffusion Flames," by D.X. Du, R.L. Axelbaum and C.K. Law, to appear in Proc. of 23rd Combustion Symposium.

4. "Experimental and Numerical Determination of Laminar Flame Speeds: Mixtures of C_2-Hydrocarbons with Oxygen and Nitrogen," by F.N. Egolfopoulos and C.K. Law, to appear in Proc. of 23rd Combustion Symposium.

5. "An Experimental and Computational Study of the Burning Rates of Ultra-Lean to Moderately-Rich $H_2/O_2/N_2$ Laminar Flames with Pressure Variations," by F.N. Egolfopoulos and C.K. Law, to appear in Proc. of 23rd Combustion Symposium.

6. "A Kinetic Criterion of Flammability Limits: The C-H-O-Inert System," by C.K. Law and F.N. Egolfopoulos, to appear in Proc. of 23rd Combustion Symposium.

7. "An Experimental and Theoretical Investigation of the Dilution, Pressure and Flow-field Effects on the Extinction Conditions of Methane-Air-Nitrogen Diffusion Flames," by H.K. Chelliah, C.K. Law, T. Ueda, M.D. Smooke and F.A. Williams, to appear in Proc. of 23rd Combustion Symposium.

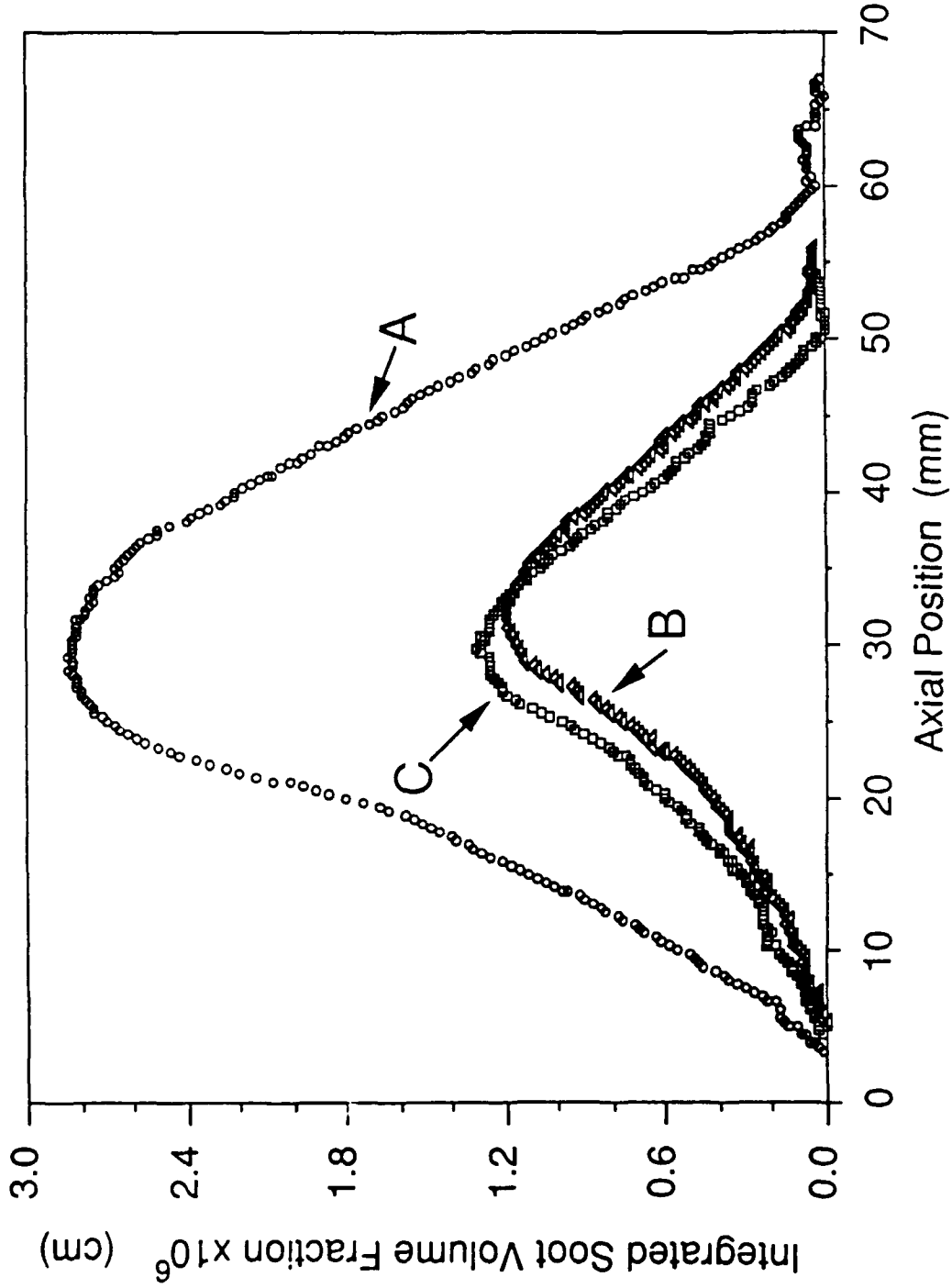
Integrated Soot Volume Fraction x10^6 (cm)
3.0
2.4
1.8
1.2
0.6
0.0
0
10
20
30
40
50
60
70
Axial Position (mm)
A
B
C

Figure 1

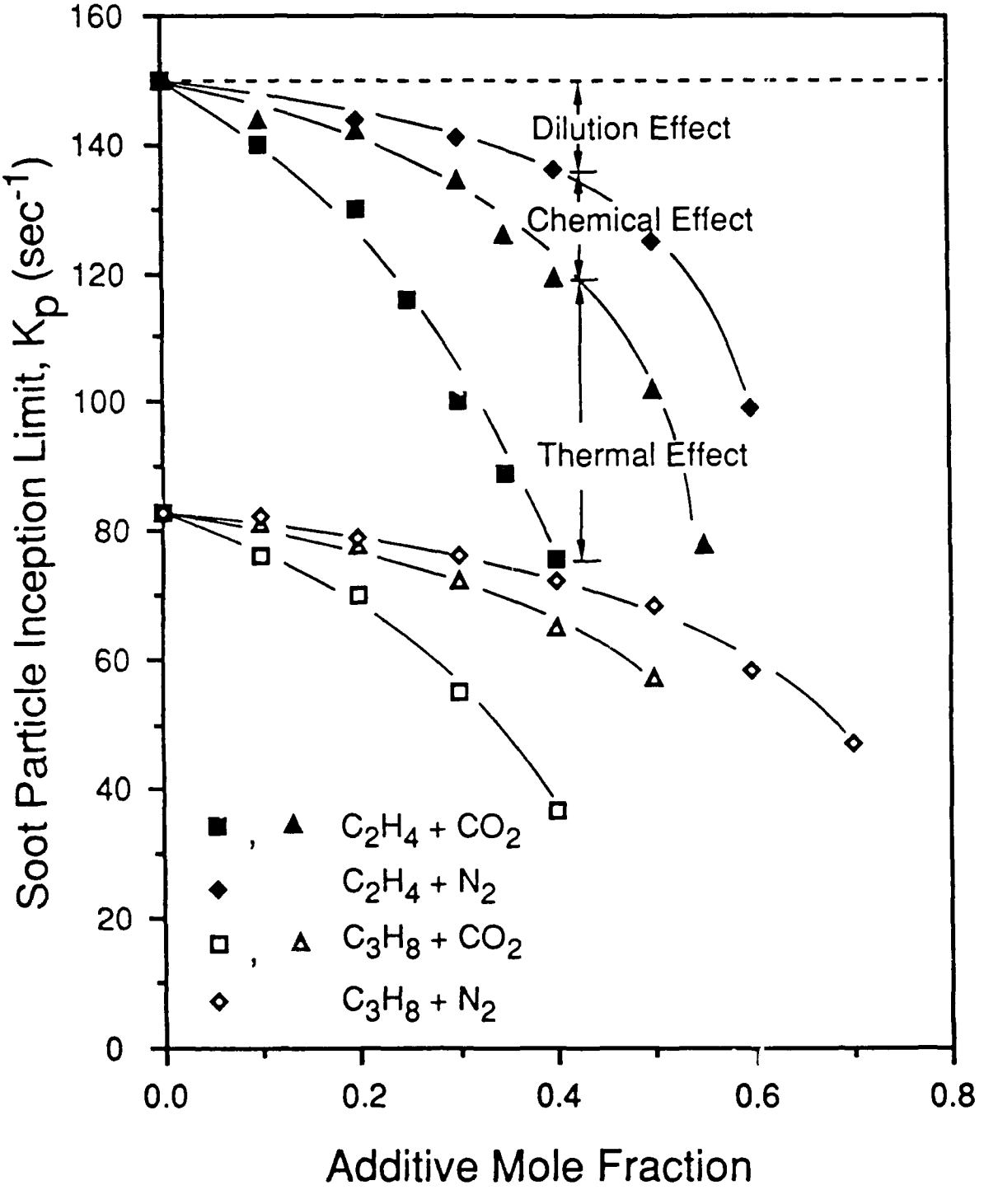
Soot Particle Inception Limit, K_p (sec^{-1})
Additive Mole Fraction
Dilution Effect
Chemical Effect
Thermal Effect
$C_2H_4 + CO_2$
$C_2H_4 + N_2$
$C_3H_8 + CO_2$
$C_3H_8 + N_2$
0
20
40
60
80
100
120
140
160
0.0
0.2
0.4
0.6
0.8

Figure 2

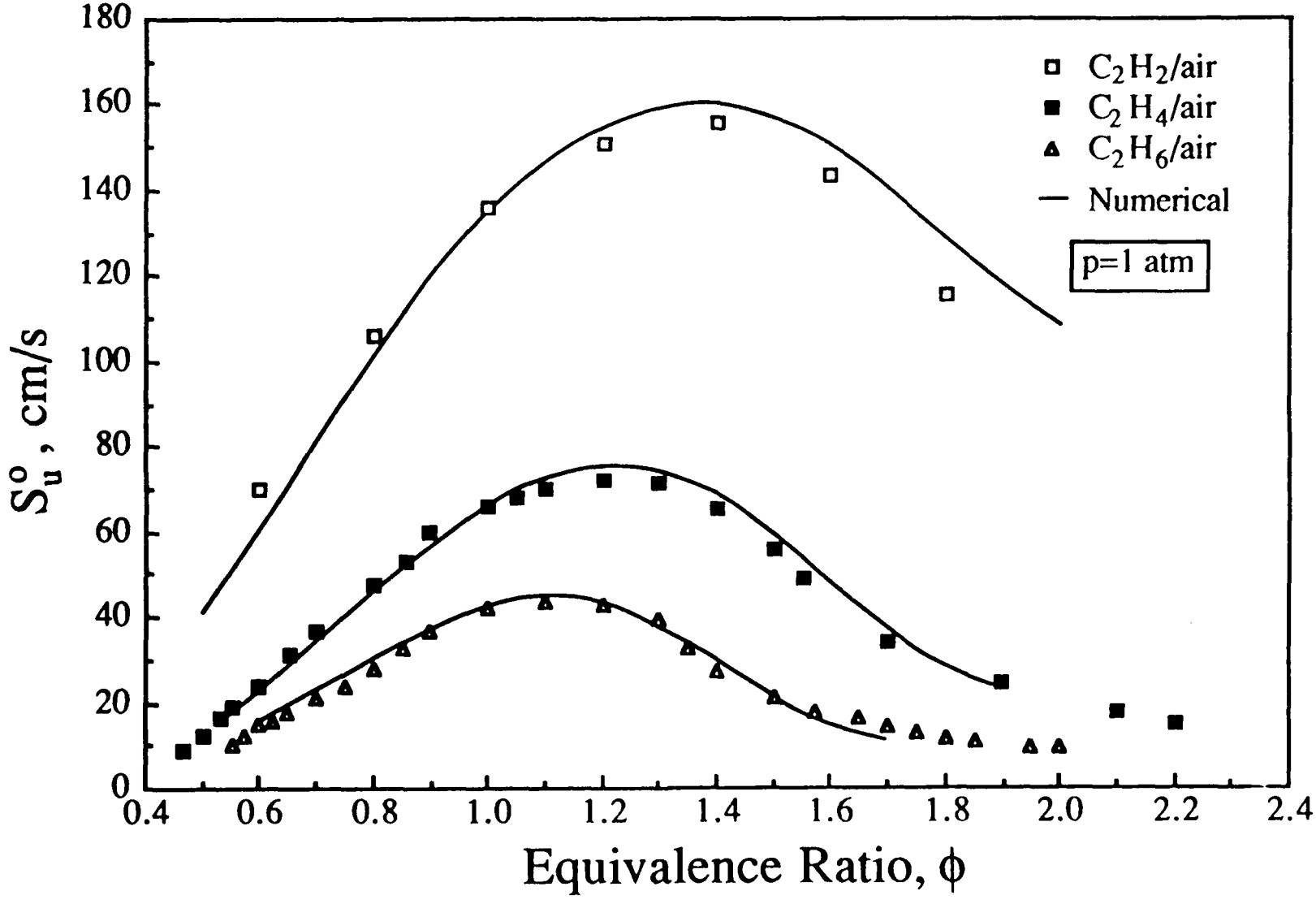
180
160
140
120
100
80
60
40
20
0
S_u^o, cm/s
0.4
0.6
0.8
1.0
1.2
1.4
1.6
1.8
2.0
2.2
2.4
Equivalence Ratio, ϕ
C_2H_2/air
C_2H_4/air
C_2H_6/air
Numerical
p=1 atm

Figure 3

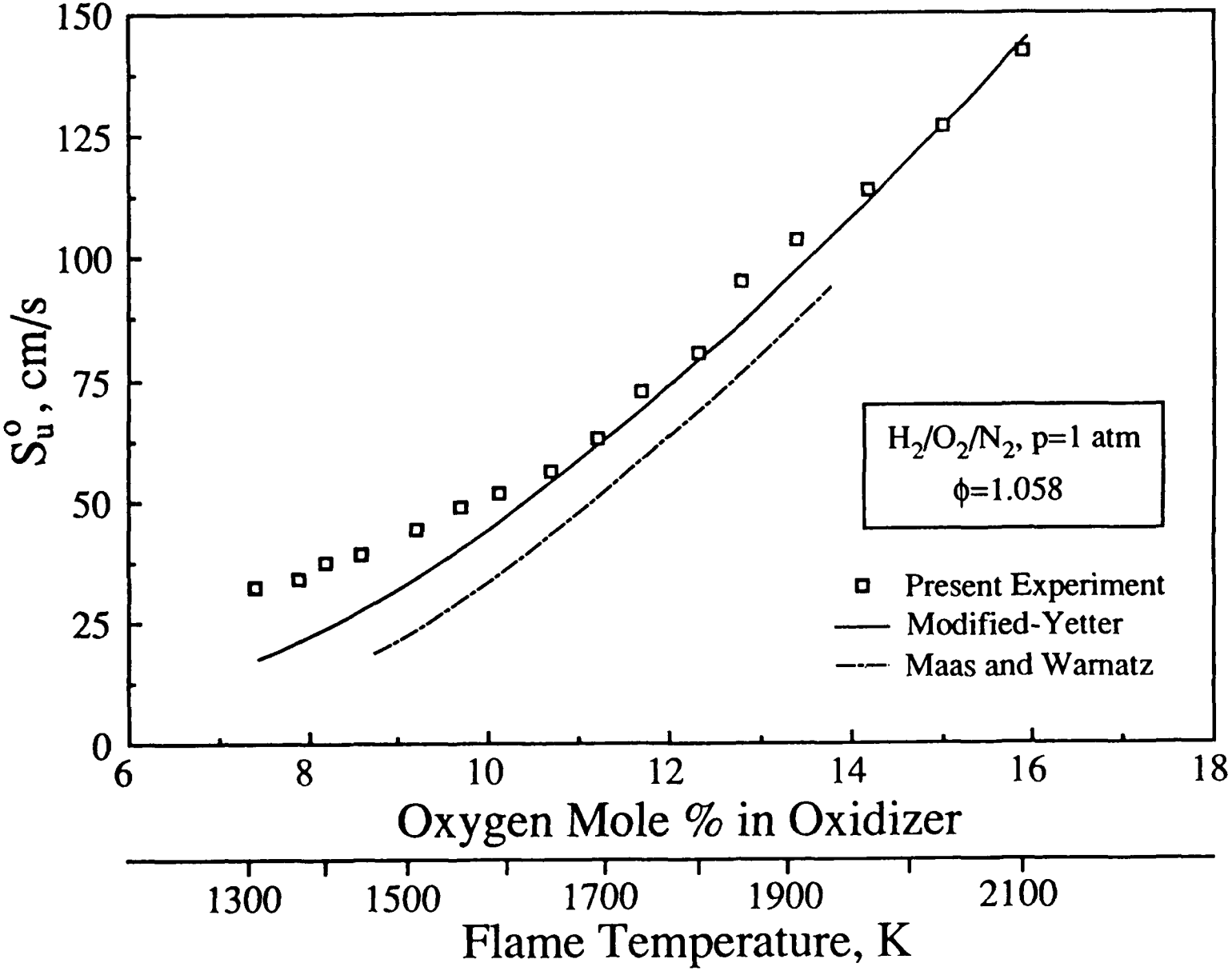
150
125
100
75
50
25
0
S_u^o, cm/s
$H_2/O_2/N_2$, p=1 atm
ϕ=1.058
Present Experiment
Modified-Yetter
Maas and Warnatz
6
8
10
12
14
16
18
Oxygen Mole % in Oxidizer
1300
1500
1700
1900
2100
Flame Temperature, K

Figure 4

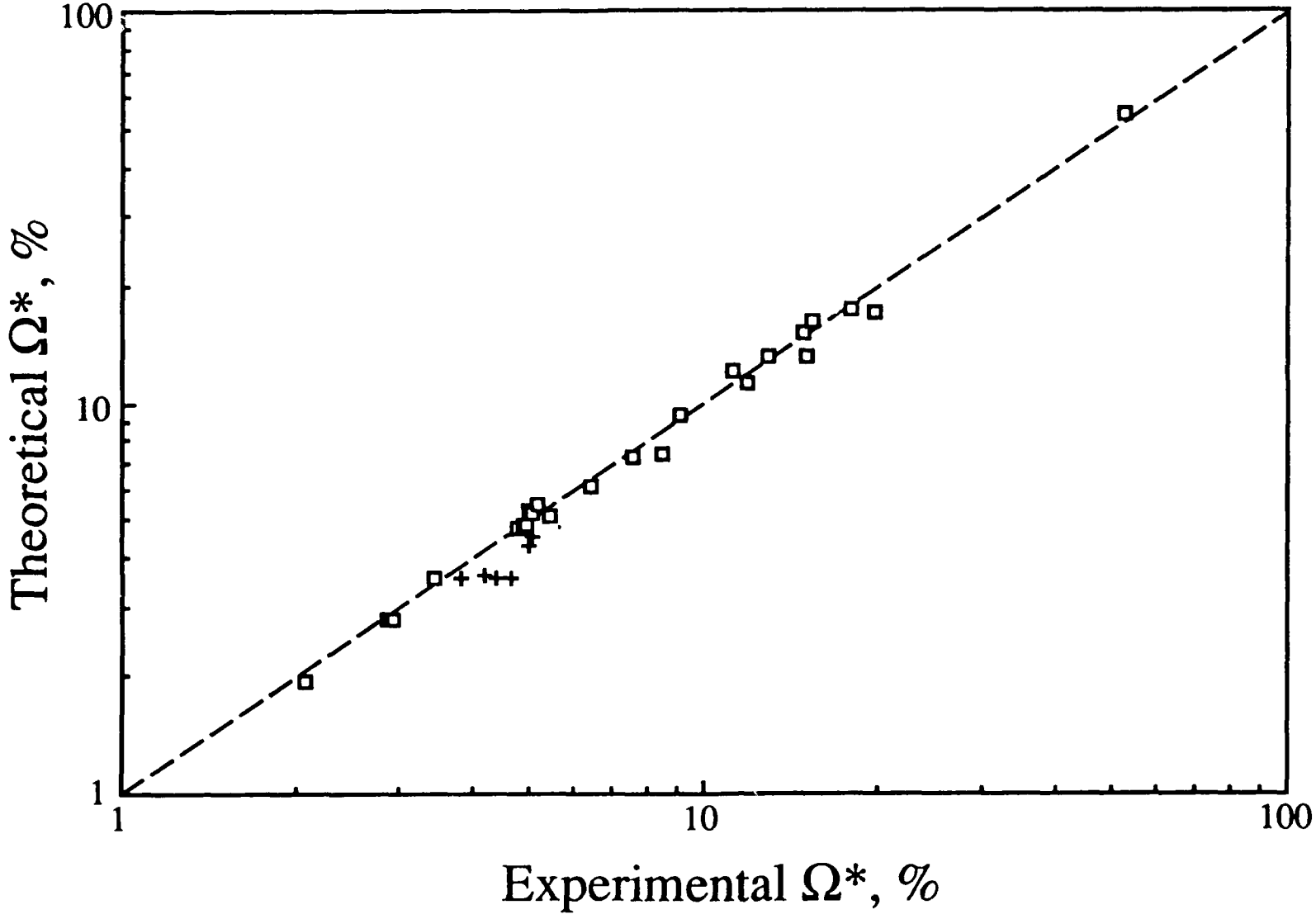

Figure 5

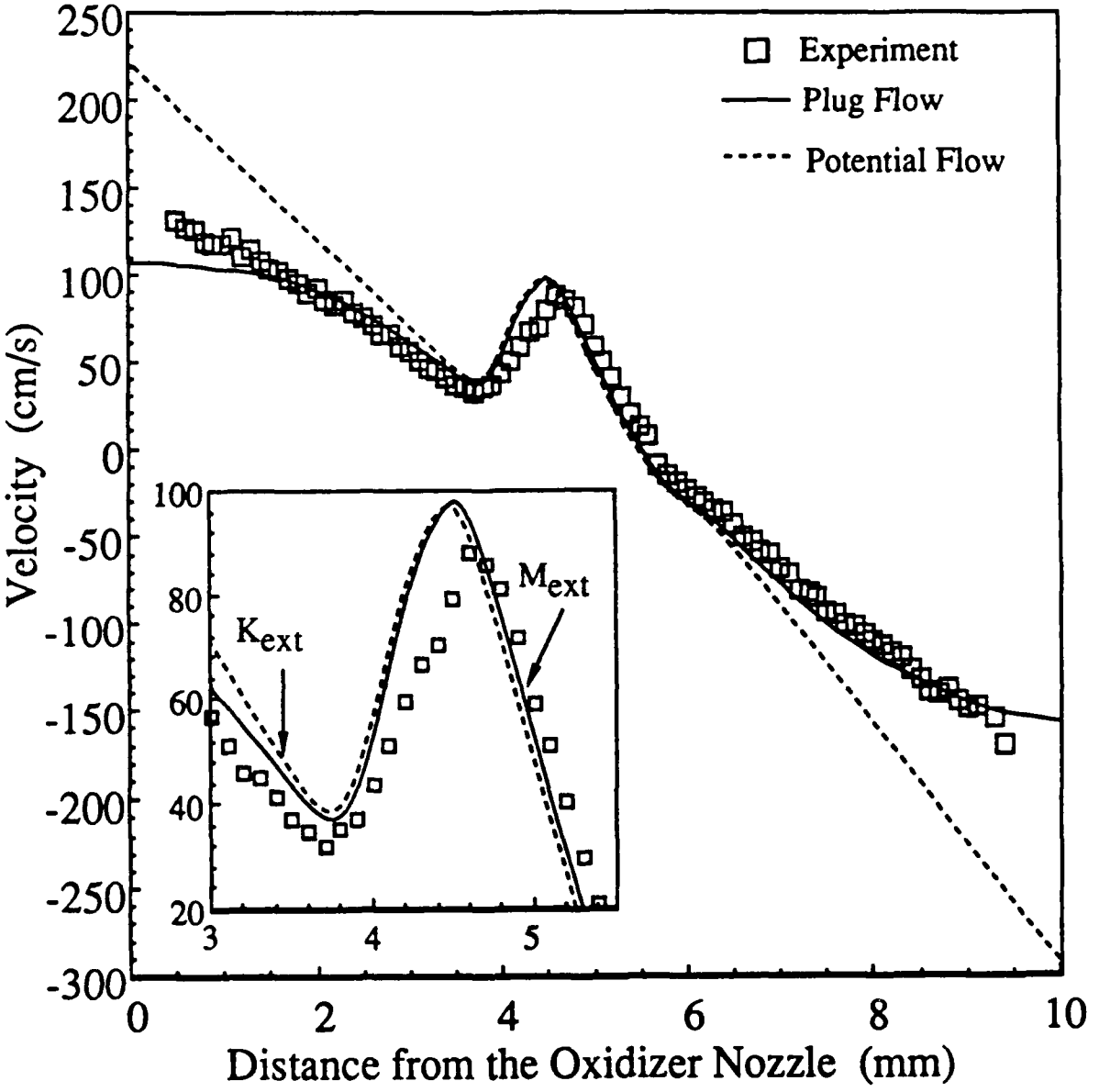
Experiment
Plug Flow
Potential Flow
Velocity (cm/s)
250
200
150
100
50
0
-50
-100
-150
-200
-250
-300
0
2
4
6
8
10
Distance from the Oxidizer Nozzle (mm)
100
80
60
40
20
3
4
5
K_{ext}
M_{ext}

Figure 6

TABLE 1

(L/R) Mixture	p, atm	Experimental Ω^* (ϕ^*)	T_{ad}, K	S_u^o, cm/s	Theoretical Ω^* (ϕ^*)
(L) CH_4/air	3.00	5.18 (0.52)	1520	----	5.46 (0.55)
(L) CH_4/air	2.00	5.08 (0.51)	1500	----	5.18 (0.52)
(R) CH_4/air	2.00	15.5 (1.75)	1727	4.0	16.1 (1.82)
(L) CH_4/air	1.00	4.80 (0.48)	1442	4.3	4.80 (0.48)
(R) CH_4/air	1.00	14.9 (1.67)	1782	5.3	15.1 (1.69)
(L) CH_4/air	0.75	4.90 (0.49)	1461	5.0	4.90 (0.49)
(L) CH_4/air	0.50	4.80 (0.48)	1481	6.0	4.80 (0.48)
(L) CH_4/air	0.375	5.08 (0.51)	1480	9.0	4.51 (0.45)
(L) CH_4/air	0.25	4.99 (0.50)	1470	11.1	4.32 (0.43)
(L) CH_4/"Ar-air "	1.0	3.45 (0.34)	1412	3.9	3.55 (0.35)
(R) CH_4/"Ar-air "	1.0	17.9 (2.07)	1771	7.5	17.4 (2.00)
(L) CH_4/[0.5925Ar+0.1975He+0.21O_2][a]	1.0	3.84 (0.38)	1525	10.4	3.55 (0.35)
(L) CH_4/[0.395Ar+0.395He+0.21O_2][a]	1.0	4.23 (0.42)	1634	20.5	3.60 (0.36)
(L) CH_4/[0.1975Ar+0.5925He+0.21O_2][a]	1.0	4.42 (0.44)	1687	31.5	3.55 (0.35)
(L) CH_4/"He-air "	1.0	4.70 (0.47)	1765	43.8	3.55 (0.35)
(L) CH_4/[0.18O_2+0.82N_2][a]	1.0	4.96 (0.58)	1477	4.7	4.88 (0.57)
(L) CH_4/[0.151O_2+0.849N_2][a]	1.0	4.95 (0.69)	1475	5.0	4.81 (0.67)
(R) CH_4/[0.151O_2+0.849N_2][a]	1.0	9.06 (1.32)	1682	4.6	9.25 (1.35)
(L) [0.94CH_4+0.06CH_3Br]/air[a]	1.0	5.42 (0.57)	1597	----	5.15 (0.54)
(L) H_2/air	1.5	6.52 (0.17)	828	----	---- (----)
(L) H_2/air	1.0	6.30 (0.16)	811	----	---- (----)
(L) H_2/air	0.5	5.74 (0.14)	767	----	---- (----)
(R) $H_2/O_2/N_2$ (ϕ=1.6)[b]	1.0	15.2 (----)	1067	7.0	13.1 (----)
(R) $H_2/O_2/N_2$ (ϕ=1.6)[b]	0.75	11.9 (----)	903	1.0	11.1 (----)
(R) $H_2/O_2/N_2$ (ϕ=1.6)[b]	0.5	8.49 (----)	736	0.5	7.43 (----)
(R) $H_2/O_2/N_2$ (ϕ=2.0)[b]	1.0	19.8 (----)	1101	12.0	16.9 (----)
(L) [0.25CH_4+0.75H_2]/air[a]	1.0	5.66 (0.25)	998	----	---- (----)
(L) [0.50CH_4+0.50H_2]/air[a]	1.0	5.10 (0.32)	1136	----	---- (----)
(L) [0.75CH_4+0.25H_2]/air[a]	1.0	5.03 (0.41)	1313	----	5.27 (0.43)
(L) C_2H_6/air	1.0	2.91 (0.50)	1506	7.2	2.80 (0.48)
(R) C_2H_6/[0.16O_2+0.84N_2][a]	1.0	7.59 (1.80)	1512	3.0	7.20 (1.70)
(L) C_2H_4/air	1.0	2.92 (0.43)	1516	5.8	2.79 (0.41)
(R) C_2H_4/[0.12O_2+0.88N_2][a]	1.0	6.44 (1.72)	1484	3.2	6.09 (1.62)
(L) C_2H_2/air	1.0	2.86 (0.35)	1400	9.0	2.78 (0.34)
(L) C_3H_8/air	1.0	2.06 (0.50)	1511	7.6	1.94 (0.47)
(L) [0.92CO+0.08H_2]/air	1.0	11.2 (0.30)	1277	1.8	11.9 (0.32)
(L) [0.92CO+0.08H_2]/[0.113O_2+0.887N_2][a]	1.0	13.0 (0.66)	1408	4.1	13.0 (0.66)
(R) [0.92CO+0.08H_2]/[0.113O_2+0.887N_2][a]	1.0	52.5 (4.90)	1245	8.5	54.0 (5.20)

[a] Species coefficients represent mole fractions in fuel and/or oxidizer mixtures.
[b] Flammability limit obtained by varying the nitrogen dilution for fixed ϕ.

COMBUSTION AND FLAME 80: 7-16 (1990)

Chain Mechanisms in the Overall Reaction Orders in Laminar Flame Propagation

F. N. EGOLFOPOULOS and C. K. LAW

Department of Mechanical and Aerospace Engineering, Princeton University, Princeton, NJ 08544

The laminar flame speeds of methane-oxygen-nitrogen mixtures as functions of the flame temperature T_{ad} and system pressure p have been experimentally determined by using the counterflow, twin-flame technique. These data are then compared with numerically-calculated values obtained by using an independently validated kinetic scheme. Results show that the overall reaction order n and activation energy E_a are far from being constants, that n decreases with increasing p and decreasing T_{ad} whereas E_a increases with increasing p, and that n can actually assume negative values; the last result implies that the mass burning rate of some weakly burning flames may decrease with increasing pressure. By further identifying the crucial reaction steps through sensitivity analysis, the present results are interpreted on the basis of the influence of chain branching-termination mechanisms on the overall reaction rate.

INTRODUCTION

Chain mechanisms, especially those involving the competition between branching and termination reactions, are of intrinsic importance to chemically reacting systems because they are potentially capable of qualitatively modifying the combustion behavior from those anticipated on the basis of, say, one-step overall reactions. Examples pertaining to purely chemical systems include the explosion limits of hydrogen-oxygen mixtures and the cool flame phenomena of hydrocarbon-air mixtures. Comparatively fewer studies, however, have been conducted on the influence of branching-termination chain mechanisms on the *global* behavior of *flames*, for which molecular transport as well as chemical kinetic processes are inherently coupled. Recently the interest and activities in this class of phenomena have increased considerably because of the increased capability to conduct detailed numerical modeling of combustion phenomena. The particular flame configuration that has been frequently adopted for such studies is the steady propagation of the adiabatic one-dimensional planar flame in the doubly-infinite domain. The flow field in this configuration is well defined and is the simplest possible, thus allowing the unambiguous exploration and identification of the influence of chemical kinetics on the flame behavior. Consequently, through numerical simulation of such flames Westbrook and Dryer [1, 2], Warnatz [3], Dixon-Lewis [4], and Coffee and co-workers [5, 6] have amply demonstrated the importance of chain mechanisms in the flame structure and propagation. It is further emphasized [1, 2] that, because of chain termination, the calculated laminar flame speed decreases with pressure at a faster rate when the pressure exceeds a certain range. Because this behavior is central to the present study, we briefly discuss the cause responsible for it.

First, a simple heat and mass balance shows that the burning rate (per unit area) of the laminar flame, m^0, is related to the overall reaction rate w through $m^0 \sim w^{1/2}$. Since for a given mixture concentration and upstream conditions we can write

$$w \sim p^n \exp(-E_a/R^0 T_{ad}), \qquad (1)$$

Published by Elsevier Science Publishing Co., Inc.
655 Avenue of the Americas, New York, NY 10010

0010-2180/90/$03.50

where p is the pressure, T_{ad} the adiabatic flame temperature, and n and E_a, respectively, the overall reaction order and activation energy pertaining to that particular mixture and burning configuration, we have

$$m^0 \sim p^{n/2} \exp(-E_a/2R^0T_{ad}). \tag{2}$$

In writing Eq. 2 it is recognized that the remaining influences of pressure and flame temperature, through transport property variations, are secondary.

The parameters n and E_a are to be empirically determined. Thus with a given set of either experimental or numerical data $m^0(p, T_{ad})$, these parameters can be defined as

$$n = 2\left\{\frac{\partial[\ln(m^0)]}{\partial[\ln(p)]}\right\}_{T_{ad}}, \tag{3}$$

$$E_a = -2R^0\left\{\frac{\partial[\ln(m^0)]}{\partial[1/T_{ad}]}\right\}_{p}. \tag{4}$$

The mass burning rate m^0 is the eigenvalue of laminar flame propagation and therefore is the proper parameter to indicate the burning intensity of the flame. However, traditionally the laminar flame speed S_u^0 has been used. Since $m^0 = \rho_u S_u^0$, Eq. 2 can be expressed in terms of S_u^0 as

$$S_u^0 \sim p^{\gamma} \exp(-E_a/2R^0T_{ad}), \tag{5}$$

where ρ_u is the density of the unburned mixture and

$$\gamma = \frac{n}{2} - 1. \tag{6}$$

Equation 6 shows that the dependence of S_u^0 on p includes the effects of both chemical reaction $(n/2)$ and density variation (-1). Thus when S_u^0 is used for data interpretation, the density effect has to be first subtracted out before inferences can be made regarding the effect of pressure on the burning intensity.

We next consider the influence of chain mechanisms on the laminar burning rate via the example

$$H + O_2 \rightarrow OH + O, \tag{B}$$

$$H + O_2 + M \rightarrow HO_2 + M, \tag{T}$$

which are two of the crucial chain branching and (quasi-) termination reaction steps in the oxidation kinetics of hydrogen and hydrocarbons. The branching step (B) is a temperature-sensitive, two-body reaction, while the termination step (T) is a temperature-insensitive, three-body reaction. Thus the branching and termination reactions can be enhanced relative to each other by increasing the flame temperature (T_{ad}) and system pressure (p), respectively. This influence should then be reflected in the overall reaction rate m^0 in that it is increased with increasing T_{ad} but is decreased with increasing p. This is the reasoning of Westbrook and Dryer [1, 2] for their numerical result of decreasing $S_u{}^0$ with increasing p. It also supports previous experimental observations: for example, Lewis [7] reported a maximum negative value of γ of about -0.4 for weakly burning flames whereas Andrews and Bradley [8] showed that for methane-air mixtures $\gamma = -0.5$ for $p > 5$ atm.

Further insight into the influence of chain mechanisms can be gained from these previous results. First, since S_u^0 is not the proper eigenvalue of laminar flame propagation when pressure variation is involved, a decreasing trend of S_u^0 with pressure, $\partial S_u^0/\partial p < 0$, does not provide direct indication of a negative kinetic influence, due to chain termination, on the burning rate of the flame. Indeed, by using Eq. 6, the previously reported γ all correspond to positive values of n, with $2 > n \geq 1$. On the other hand, the facts that these n values are smaller than 2, that n also decreases with pressure, and that removal of the termination reaction (T) changes the value of n, as pointed out by Westbrook and Dryer [1, 2], do indicate the progressive importance of termination reactions with pressure. That is, since a strongly burning flame, dominated by two-body branching and carrying reactions, should have an n close to 2, results of n substantially smaller

than 2 indicate the possible, simultaneous importance of the three-body termination reactions that generally tend to reduce n, and of the first-order unimolecular decomposition reactions as the high-pressure limit of the Lindemann mechanism. The relative importance of the unimolecular reactions as compared to the termination reactions can be further eliminated because, if they were important, n would increase with pressure, indicating the progressive dominance of the two-body propagation reactions. Thus it can be concluded that the previous results of $2 > n \geq 1$ and n decreasing with pressure do provide strong evidence of the importance of the three-body termination reactions in the flame burning intensity.

The present study aims to extend these previous, worthwhile contributions along the following directions. First, in view of the recent recognition that previous experimental determination of the laminar flame speeds could have been complicated by stretch effects [9], we shall perform accurate determinations of S_u^0 of methane–O_2–N_2 mixtures as functions of pressure by using the recently developed counterflow technique [10–14] in which stretch effects are systematically subtracted out. The increased accuracy is especially important for the slow-burning flames of interest in this study, as is further discussed in the next section.

We shall also determine S_u^0 as function of the flame temperature, which yields values of the overall activation energy. Very little accurate experimental data exist for this parameter.

In addition to the experimental investigations, we shall perform numerical simulations of these flames by using a kinetic scheme independently validated for flame speed calculations, and compare the calculated values with our experimental data. Very close agreement is obtained, thereby providing confidence in the accuracy of the present study as well as the meaningfulness of the insights gained herein.

An auxiliary objective of the present study is to explore the possible existence of reaction regimes in which the termination reactions are so strong that the overall reaction orders may assume values of $n < 1$ or even $n < 0$. The need for such an exploration is that it is not clear a priori whether such weakly burning flames can indeed exist. If they do not exist, then the range of possible values of n is significantly narrowed. This can lead to considerable simplifications in the extent of investigation in future parametric and modeling studies. On the other hand, if they do exist, especially the $n < 0$ situations for which the mass burning rate decreases with increasing pressure, then their significance should be recognized and accounted for in future efforts.

The experimental and numerical aspects of the present investigation are respectively presented in the next two sections.

EXPERIMENTAL METHODOLOGY AND RESULTS

The experiment adopts the counterflow technique of Law and co-workers [10–14] in determining the flame speed. It basically involves the establishment of two symmetrical, planar, nearly adiabatic flames in a nozzle-generated counterflow configuration, and determining the axial velocity profile along the centerline of the flow by using LDV. The minimum point of the velocity profile can be identified as a reference upstream flame speed S_u, with the velocity gradient ahead of it as the imposed stretch rate K. Thus by plotting S_u versus K, we can obtain the stretch-free flame speed S_u^0 through linear extrapolation to $K = 0$. The entire burner is housed in a large strainless-steel chamber with continuous air ventilation, thereby allowing for pressure adjustments. Details of the experimental setup can be found in Refs. 12 and 13.

Accuracy of the present methodology is mainly limited by the uncertainty associated with velocity measurements, and is typically between 0.5 and 1.5 cm/s. This uncertainty range is generally smaller than, or of the same magnitude as, the size of the data symbols shown in the following figures. Thus error bars are not shown.

This methodology is well-suited for the present investigation of pressure effects on weakly burning flames. This is because the conventional method in studying pressure effects on flames speeds is that of the expanding spherical flame in an enclosed bomb. For these spherical flames it is well recognized that experimental accuracy is low during the

initial period when effects of flame curvature and heat loss to the electrodes are significant. Furthermore, as the flame grows larger and data can be normally taken, buoyancy will have caused severe distortion and upward displacement of the flame ball configuration for weakly burning flames. Heat loss to the electrodes may still be important at this stage because these flames are extremely weak. It is therefore clear that accurate flame speed data cannot be readily determined or unambiguously extracted by using the spherical flame methodology.

For the present counterflow methodology, upstream heat loss is minimized because the flow is nozzle-generated and downstream heat loss is minimized due to symmetry. The buoyancy effects are automatically included in that the LDV-velocity profile is the *local* value experienced by the specific flame segment (around the stagnation point) under measurement; in the Appendix we provide further discussion and experimental data that substantiate this statement. This methodology is therefore ideally suited for the present experiment.

Methane-oxygen-nitrogen flames will be studied because this is the only hydrocarbon fuel whose oxidation scheme has been extensively investigated and reasonably well established as far as the flame speed calculation is concerned. Thus there is reasonable confidence in comparing the experimental data with the numerical calculations for these flames.

Two series of experiments were conducted. The first involved methane-air mixtures with different equivalence ratios, ϕ, and at different pressures. Thus for a given ϕ, differentiation of m^0 with p according to Eq. 3 yields n. A similar determination of E_a by differentiating m^0 by T_{ad} according to Eq. 4, however, is less meaningful because of the simultaneous influence of ϕ and T_{ad} on m^0. This ambiguity is removed in the second series of experiments in which the methane-oxygen stoichiometry is fixed, at $\phi = 1$, and T_{ad} is varied by changing the nitrogen concentration. Thus by also varying the pressure, n and E_a can be determined according to Eqs. 3 and 4. Calculated T_{ad} for the various mixtures are given in Tables 1 and 2.

Figure 1 shows the experimentally determined laminar flame speeds of stoichiometric and lean

TABLE 1

Calculated Adiabatic Flame Temperatures (K) of Methane-Air Mixtures

	Equivalence Ratio (ϕ)				
P(atm)	0.6	0.8	1.0	1.2	1.4
0.25	1668	1996	2197	2130	1977
0.5	1668	2000	2215	2135	1979
1.0	1669	2003	2232	2138	1980
1.5	1669	2005	2241	2139	1980
2.0	1669	2006	2247	2140	1980
2.5	1669	2007	2251	2141	1981
3.0	1669	2007	2254	2141	1981
3.5	1669	2008	2257	2142	1981
4.0	1669	2008	2260	2142	1981
4.5	1669	2008	2262	2142	1981

methane-air mixtures with different equivalence ratios and pressures. The results qualitatively agree with the numerical calculations of Westbrook and Dryer [1, 2] in that S_u^0 decreases monotonically with increasing pressure.

In Fig. 2a the S_u^0 is converted to the laminar burning rate $m^0 = \rho_u S_u^0$, which, as discussed previously, is a more direct parameter representing the rate of the overall chemical reaction. It is seen that m^0 now increases with pressure for all values of ϕ. By fitting these data and then differentiating the fitted results according to Eq. 3, the overall reaction orders n have been computed and are shown in Fig. 2b. The fitting was performed

TABLE 2

Calculated Adiabatic Flame Temperatures (K) of Stoichiometric Methane-Oxygen-Nitrogen Mixtures

	N_2 (%)				
P(atm)	79	82	83	84	85.6
1.0	2232	2069	2004	1936	1819
1.5	2241	2074	2007	1938	1820
2.0	2247	2077	2009	1939	1820
2.5	2251	2079	2010	1940	1821
3.0	2254	2080	2012	1941	1821
3.5	2257	2082	2012	1942	1821
4.0	2260	2083	2013	1942	1822
4.5	2262	2084	2014	1943	1822

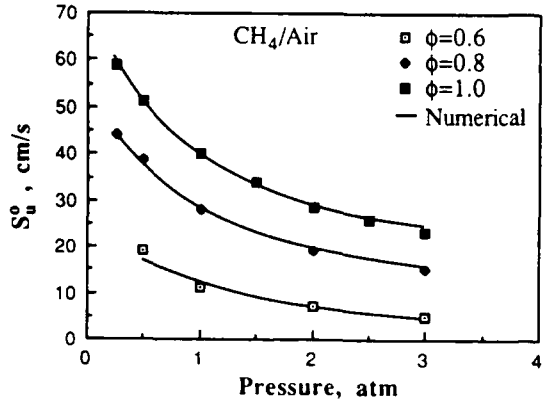

Fig. 1. Experimentally and numerically determined laminar flame speeds, S_u^0, of lean methane-air mixtures as functions of stoichiometry and pressure.

by using either graphical interpolation or second- and third-order polynomial and logarithmic functions. The results demonstrate the following points regarding the relative influence of termination versus branching reactions in the chain mechanism:

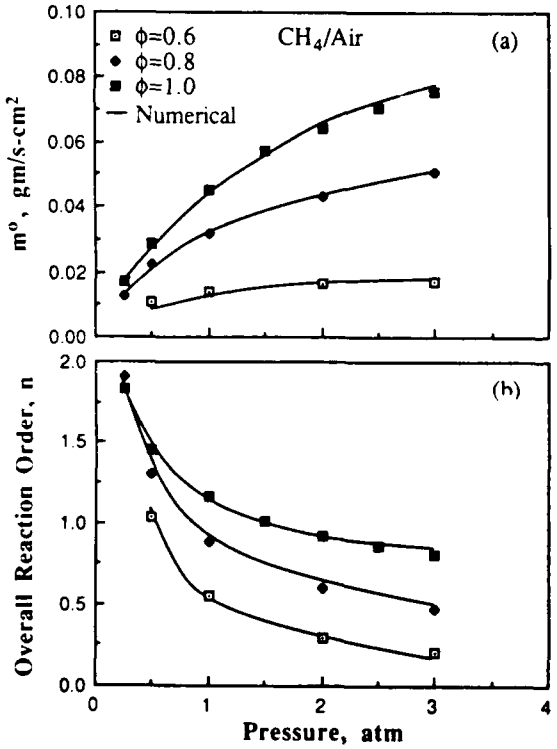

Fig. 2. Experimentally and numerically determined (a) mass burning rates, m^0, and (b) overall reaction orders, n, of lean methane-air mixtures as functions of stoichiometry and pressure.

(1) Termination reactions are enhanced with increasing pressure, hence the decreasing trend of n with p for fixed ϕ. (2) Branching reactions are weakened with decreasing ϕ, hence the decreasing n with decreasing ϕ for fixed p. (3) n approaches 2 only for very low pressures, indicating the possibility that $n \approx 2$ could be the maximum value of the reaction order for this class of mixtures, for which the two-body branching and carrying reactions represent the highest molecularity of those elementary reactions that have positive influence on the overall reaction rate. (4) In view of (3), it is reasonable that with increasing pressure n decreases rapidly from 2 such that it is already close to unity even for the normally robustly burning stoichiometric mixture at 1 atm. (5) The decrease in n, however, slows down after a certain pressure range. This agrees with the previous result [8] of a constant $n(=1)$ for $p > 5$ atm for the stoichiometric mixture. The slightly different value of the present n, when extrapolated to 5 atm, is not surprising considering the uncertainties associated with previous measurements. (6) This set of data does not show negative values of n, although n does become quite close to zero for the very lean situations of $\phi = 0.6$.

Figures 3 and 4 show the corresponding data for rich methane-air mixtures. The general behavior is similar to those of the lean mixtures, except that n appears to be somewhat insensitive to the stoichiometry, at least for the two cases studied.

To further explore the possible existence of neg-

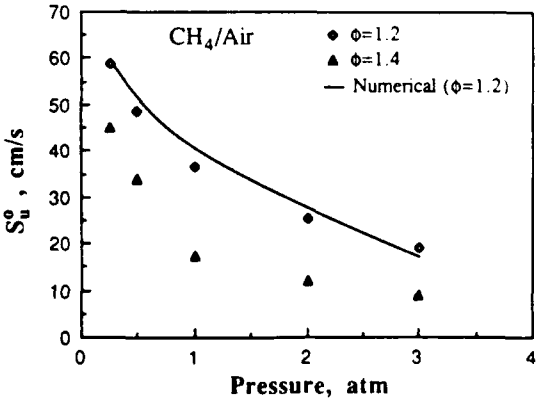

Fig. 3. Experimentally and numerically determined laminar flame speeds, S_u^0, of rich methane-air mixtures as functions of stoichiometry and pressure.

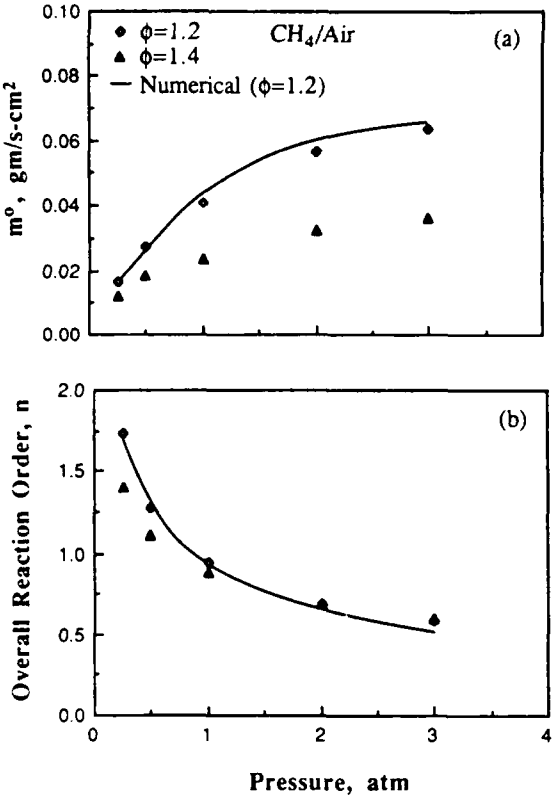

Fig. 4. Experimentally and numerically determined (a) mass burning rates, m^0, and (b) overall reaction orders, n, of rich methane-air mixtures as functions of stoichiometry and pressure.

ative n, Figs. 5 and 6 show variations of S_u^0, m^0, and n with pressure for stoichiometric mixtures with different amounts of nitrogen dilution in the $(N_2 + O_2)$ mixture. Figure 6 demonstrates clearly that although n remains positive for slightly diluted mixtures, it can indeed assume negative values for the highly diluted mixtures as pressure increases.

The data of Fig. 6a are replotted in Fig. 7 to show the dependence of m^0 on T_{ad}. It is seen that for a given pressure an approximate Arrhenius relation exists over the broad adiabatic flame temperature range of about 1820 to 2250 K (Table 2). From these relations the overall activation energies can be plotted as a function of pressure for the stoichiometric mixture, as shown in Fig. 8. It is seen that E_a increases from about 51.5 kcal/mol at 1 atm to 75.1 kcal/mol at 3 atm. Recognizing the progressive importance of the termination reac-

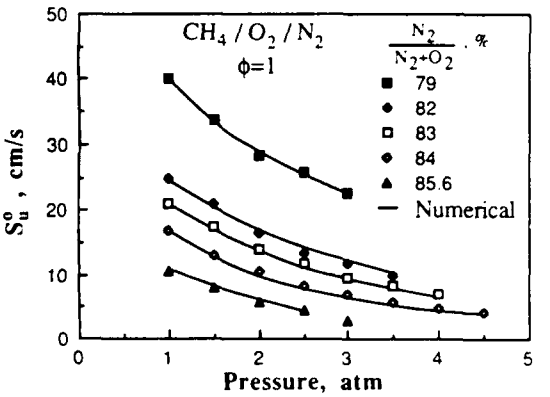

Fig. 5. Experimentally and numerically determined laminar flame speeds, S_u^0, of diluted stoichiometric methane-oxygen-nitrogen mixtures as functions of stoichiometry and pressure.

tions and thereby the increased difficulty for reactions to proceed as pressure increases, the increasing trend of E_a is reasonable. It is also significant to note the very large values of E_a for the weakly burning mixtures under elevated pressures.

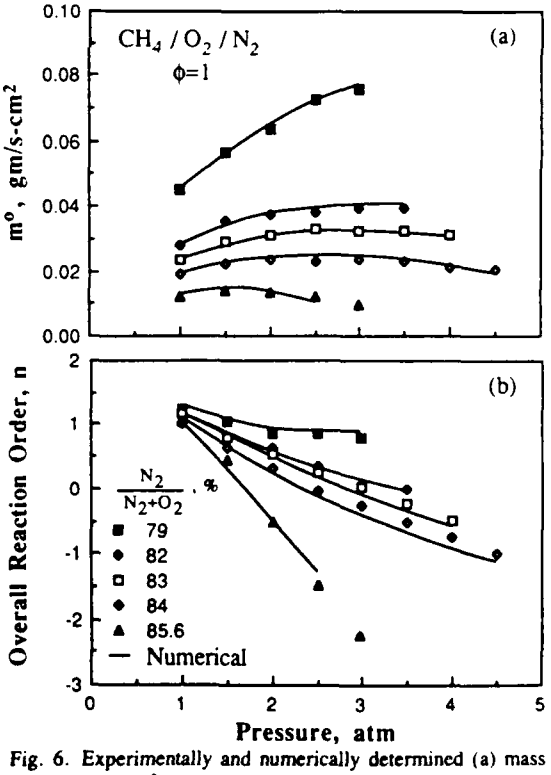

Fig. 6. Experimentally and numerically determined (a) mass burning rates, m^0, and (b) overall reaction orders, n, of diluted stoichiometric methane-oxygen-nitrogen mixtures as functions of inert dilution and pressure.

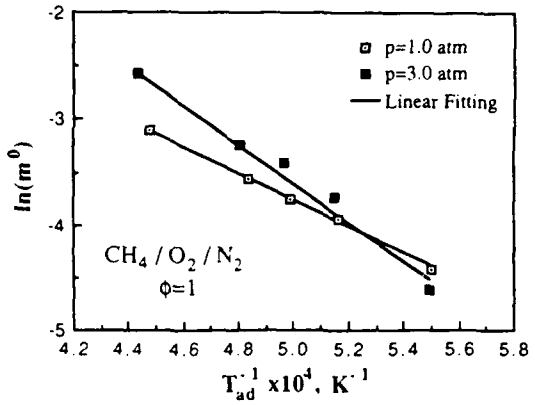

Fig. 7. Arrhenius plot of the laminar burning rate of the diluted, stoichiometric methane-oxygen-nitrogen flames.

NUMERICAL SIMULATION AND COMPARISON WITH EXPERIMENTAL DATA

In order to calculate the flame speed S_u^0 and perform the sensitivity analysis, we used the flame code of Refs. 15 and 16 with a small improvement in the computation of the mass diffusion coefficient [13]. The kinetic scheme used is the C_1-mechanism of Kee et al. [16], with 17 species and 58 reactions. This scheme has been extensively tested and validated, over wide ranges of stoichiometry, pressure, and flame temperature [14], for flame speed calculations of lean to slightly rich methane-oxygen-inert mixtures. Selected calculations have also been performed by using the full C_2-mechanism of Warnatz [17]; the results show practically no influence on the calculated flame speeds as well as the understanding and conclusions drawn herein.

The calculated results are compared with almost all of the experimental data of Figs. 1-8; the only exceptions are those for which numerical convergence becomes excessively difficult. The close agreement in the comparison is apparent. Of particular significance is the result that negative overall reaction orders are also exhibited by the numerical simulation. Because the numerical code and kinetic scheme have been previously validated for flame speed calculations, such close agreements, over the extensive range of parametric variations, strongly support the accuracy of the experimental data and thereby the viability of the present finding.

From the calculated temperature profiles the laminar flame thickness δ^0 can also be determined. Adopting the definition of Ref. 18, the calculated δ^0 for the $\phi = 1$, diluted flames are shown in Fig. 9. Comparing with Fig. 6a, the results demonstrate the anticipated relation

$$\delta^0 \sim \frac{1}{m^0}.$$

Specifically, for the highly diluted situations it is seen that δ^0 first decreases and then increases with p, just as m^0 first increases and then decreases with p.

To further identify the specific elementary re-

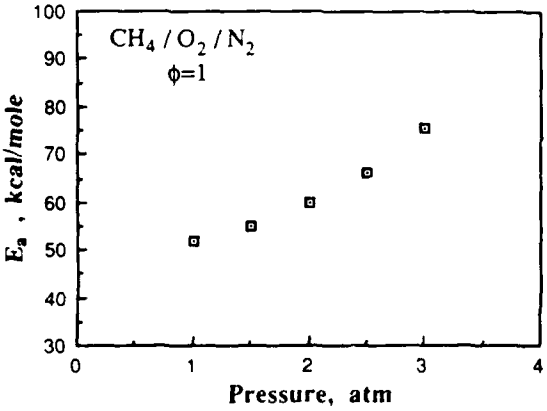

Fig. 8. Experimentally determined overall activation energies of diluted, stoichiometric methane-oxygen-nitrogen flames.

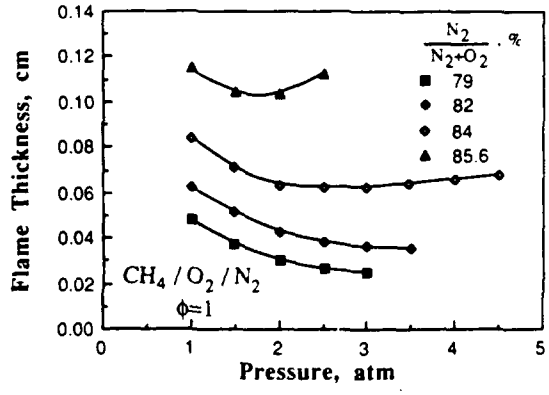

Fig. 9. Numerically determined laminar flame thicknesses, δ^0, of diluted, stoichiometric methane-oxygen-nitrogen flames.

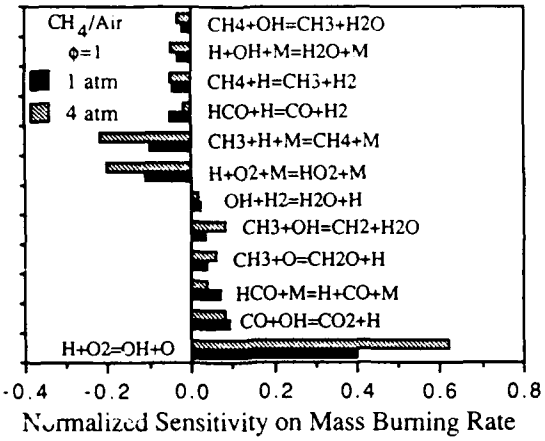

Fig. 10. Normalized sensitivities on mass burning rate for stoichiometric methane-air flames at 1 and 4 atm.

actions that are responsible for the observed behavior, Figs. 10 and 11 show the calculated sensitivities [15, 16] of the flame burning rates on the various elementary reactions for the CH_4–O_2–N_2, $\phi = 1$ mixtures, with $N_2 = 79$ and 84% and $p = 1$ and 4 atm. The results show that the dominant branching reaction is (B) as anticipated. There are two termination reactions of approximately equal importance, namely reaction (T) and

$$CH_3 + H + M \rightarrow CH_4 + M, \qquad (T')$$

which eliminates both the CH_3 and the H radicals.

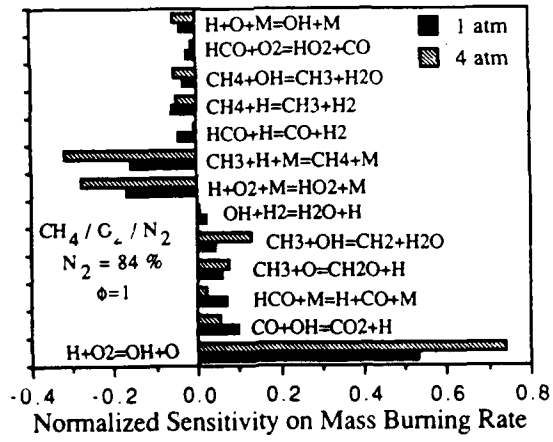

Fig. 11. Normalized sensitivities on mass burning rate for diluted stoichiometric methane-oxygen-nitrogen flames at 1 and 4 atm.

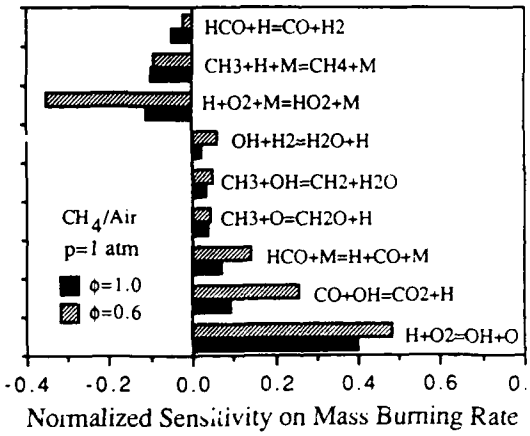

Fig. 12. Normalized sensitivities on mass burning rate for atmospheric-pressure methane-air flames with $\phi = 0.6$ and 1.0.

Figure 12 shows the sensitivities for the 1-atm methane-air flames with $\phi = 0.6$ and 1.0. It is seen that although (T) and (T′) are both important at $\phi = 1.0$, only (T) remains to be the dominant termination reaction at $\phi = 0.6$. This explains the result that although n remains positive for the $\phi = 0.6$, methane-air flame, it assumes negative values for the $\phi = 1$, 84%-diluted methane–O_2–N_2 flames even though the latter have higher flame temperatures. That is, in the former case there is only one dominant termination reaction to slow down the overall reaction rate, whereas in the latter case there are two of them.

Finally, in Figs. 13 and 14 we have plotted the

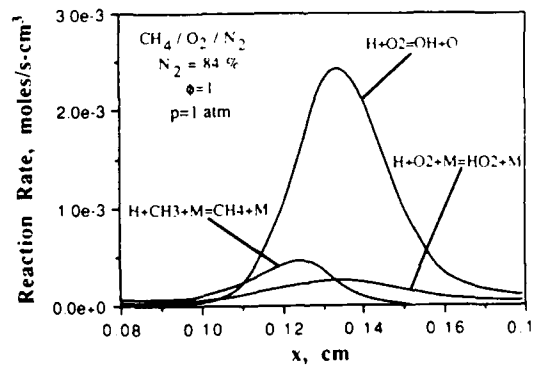

Fig. 13. Numerically calculated reaction-rate profiles of several important branching-termination reactions for diluted, stoichiometric methane-oxygen-nitrogen flames at 1 atm.

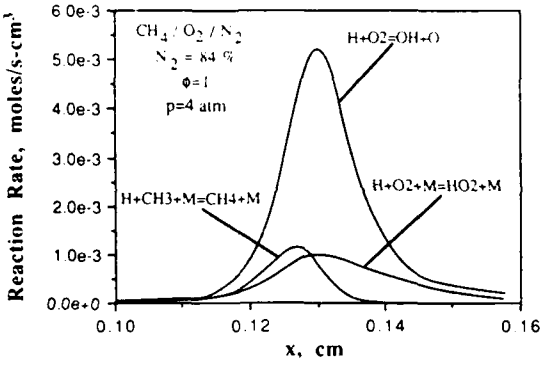

Fig. 14. Numerically calculated reaction-rate profiles of several important branching-termination reactions for diluted, stoichiometric methane-oxygen-nitrogen flames at 4 atm.

reaction rate profiles for the three dominant chain reactions for the 84%-diluted flames, at 1 and 4 atm, respectively. The results show that with increasing pressure the rates of the termination reactions increase faster than that of the branching reaction, thus further substantiating the importance of the competition between the branching and termination reactions in the flame behavior.

CONCLUDING REMARKS

In the present investigation we have experimentally determined the flame speeds of nearly adiabatic, stretch-free methane-oxygen-nitrogen flames that are subjected to variations in the flame temperature and system pressure. The viability of these data is further substantiated by their close agreement with the numerically calculated values obtained by using a kinetic scheme previously validated for the determination of flame speeds. The availability of these data of high degree of accuracy not only is required for the present study but is also useful for future modeling efforts.

Thus by analyzing the variations of the overall reaction order and activation energy with pressure and flame temperature, and by using numerical sensitivity analysis, the importance of termination reactions in the overall reaction scheme is demonstrated and quantified. The influence is substantial for practically all of the situations studied, including the standard, stoichiometric, atmospheric pressure case, and is especially significant for the weakly burning, highly diluted, elevated-pressure flames that are relevant to flame extinction and stabilization under critical conditions. It is emphasized that caution is needed in modeling efforts that use a one-step overall reaction with constant reaction order and activation energy, because the results can be quantitatively modified and sometimes even qualitatively affected when the reaction order changes sign.

FNE and CKL were respectively supported by the Air Force Office of Scientific Research under Grant AFOSR-85-0147 and the technical management of Dr. J. M. Tishkoff, and by the Department of Energy under Contract DE-FG05-87ER75362 and the technical management of Dr. M. C. Yuen.

REFERENCES

1. Westbrook, C. K., and Dryer, F. L., *Combust. Sci. Technol.* 27:31 (1981).
2. Westbrook, C. K., and Dryer, F. L., *Combust. Flame* 37:171 (1980).
3. Warnatz, J., *Eighteenth Symposium (International) on Combustion*, The Combustion Institute, Pittsburgh, 1981, p. 369.
4. Dixon-Lewis, G., *Philos. Trans. R. Soc. Lond. A* 292:45 (1979).
5. Coffee, T. P., Kotlar, A. J., and Miller, M. S., *Combust. Flame* 54:155 (1983).
6. Coffee, T. P., Kotlar, A. J., and Miller, M. S., *Combust. Flame* 58:59 (1984).
7. Lewis, B., *Selected Combustion Problems (AGARD)*, Butterworth, London, 1954, p. 177.
8. Andrews, G. E., and Bradley, D., *Combust. Flame* 19:275 (1972).
9. Law, C. K., *Twenty-Second Symposium (International) on Combustion*, The Combustion Institute, Pittsburgh, 1989, p. 1381.
10. Wu, C. K., and Law, C. K., *Twentieth Symposium (International) on Combustion*, The Combustion Institute, Pittsburgh, 1985, p. 1941.
11. Yu, G., Law, C. K., and Wu, C. K., *Combust. Flame* 63:339 (1986).
12. Law, C. K., Zhu, D. L., and Yu, G., *Twenty-First Symposium (International) on Combustion*, The Combustion Institute, Pittsburgh, 1987, p. 1419.
13. Egolfopoulos, F. N., Cho, P., and Law, C. K., *Combust. Flame* 76:375 (1989).
14. Zhu, D. L., Egolfopoulos, F. N., and Law, C. K., *Twenty-Second Symposium (International) on Combustion*, The Combustion Institute, Pittsburgh, 1989, p. 1537.
15. Grcar, J. F., Kee, R. J., Smooke, M. D., and Miller, J. A., *Twenty-First Symposium (International) on Com-*

bustion, The Combustion Institute, Pittsburgh, 1986, p. 1773.
16. Kee, R. J., Grcar, J. F., Smooke, M. D., and Miller, J. A., Sandia Report SAND85-8240, 1985.
17. Warnatz, J., *Combustion Chemistry* (W. C. Gardiner, Jr., Ed.), Springer Verlag, New York, 1984, pp. 197-360.
18. Tsatsaronis, G., *Combust. Flame* 33:217, (1978).
19. Williams, F. A., *Combustion Theory*, 2nd ed., Benjamin-Cummings, Menlo Park, CA, 1985.

Received 9 January 1989; revised 10 May 1989

APPENDIX: INFLUENCE OF BUOYANCY ON FLAME SPEED DETERMINATION

To assess the influence of buoyancy on the accuracy of the counterflow methodology in flame speed determination, especially for weak flames, we first note that buoyancy itself does not directly affect energy and species transport [19]. Indirectly, it modifies the flow field through momentum transport, and consequently the flame response.

Experimentally, buoyancy could displace the twin-flame ensemble upward relative to the symmetry plane. However, since the LDV measurements are local values, the modification of the flow field is automatically accounted for in the measured values. To substantiate this statement, Fig. A1 shows the centerline velocity profile of a 1-atm, weakly burning ($\phi = 0.60$), CH_4-air flame ensemble. It is seen that the velocity profiles for the upper and lower flames are quite symmetrical. In Fig. A2 we plot the reference, stretched flame speed S_u versus the stretch rate K to yield S_u^0 at $K = 0$ through extrapolation. It is clear that the difference in the S_u^0 determined is within the range of experimental uncertainty stated previously.

We emphasize that the key ingredients that make the present methodology a useful one are (1) the measurements are local values, and (2) extrapolation to zero stretch eliminates all the stretch effects, whether they are intentionally imposed, or inadvertently present. As a corollary, we caution against the use of the bulk stretch rate, obtained from information on the nozzle separation distance and the exit velocity, to quantify the effect of stretch on flames.

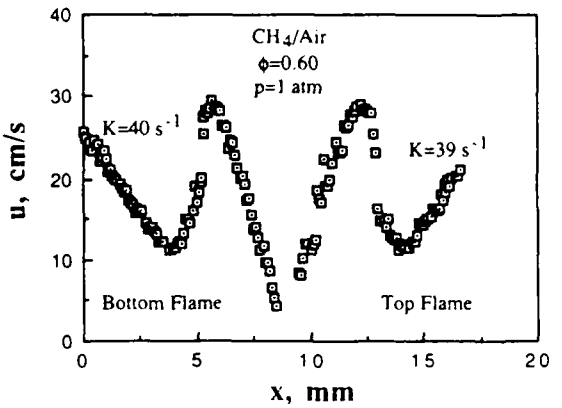

Fig. A1. Experimentally determined velocity field between the two nozzles for a CH_4-air twin-flame ensemble with $p = 1$ atm and $\phi = 0.6$.

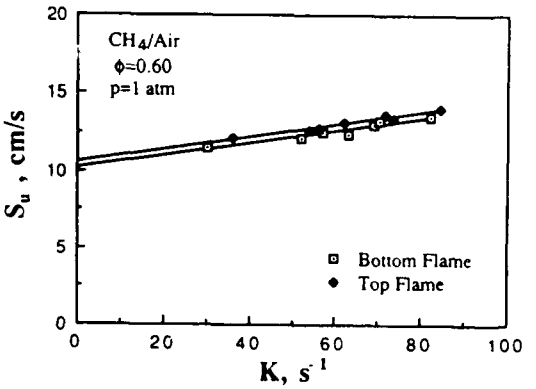

Fig. A2. Reference, stretched flame speed as a function of local stretch rate for the upper and lower flames.